

Supplementary Materials

Pt_xNi_{10-x}O Nanoparticles Supported on N-doped Graphene Oxides with A Synergetic Effect for Highly Efficient Hydrolysis of Ammonia Borane

Binhua Zhao,^{a,1} Kun Feng,^{a,1} Yun Wang,^a Xiaoxin Lv,^a Hechuang Zheng,^a Yanyun Ma,^{a,} Wensheng Yan,^b Xuhui Sun,^{a,*} and Jun Zhong^{a,*}*

^a Institute of Functional Nano and Soft Materials Laboratory (FUNSOM), Jiangsu Key Laboratory for Carbon-Based Functional Materials & Devices, Soochow University, Suzhou 215123, China

^b National Synchrotron Radiation Laboratory, University of Science and Technology of China, Hefei, Anhui 230029, China

¹ The two authors have equal contribution to this work.

* **Address correspondence to** mayanyun@suda.edu.cn (Y. Ma); xhsun@suda.edu.cn (X. Sun);

jzhong@suda.edu.cn (J. Zhong)

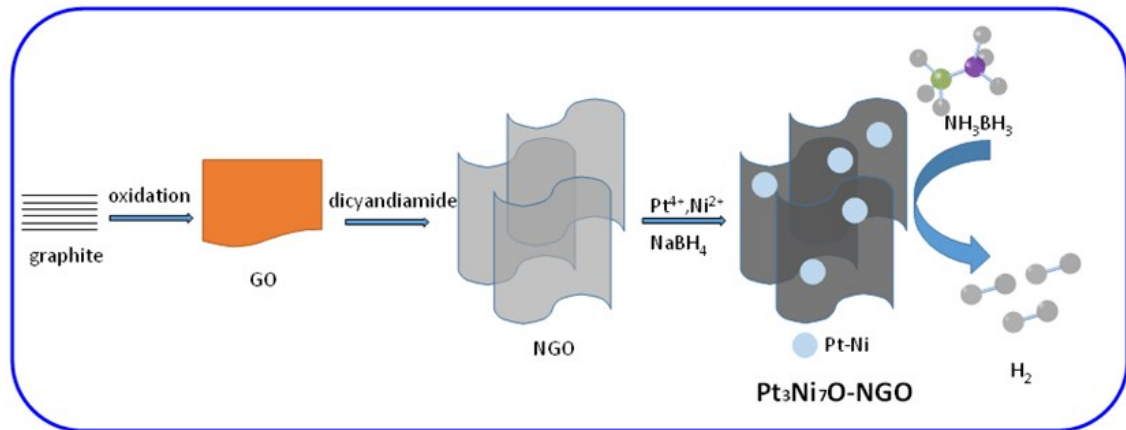


Fig. S1. Illustration of the preparation processes for the Pt₃Ni₇O-NGO sample.

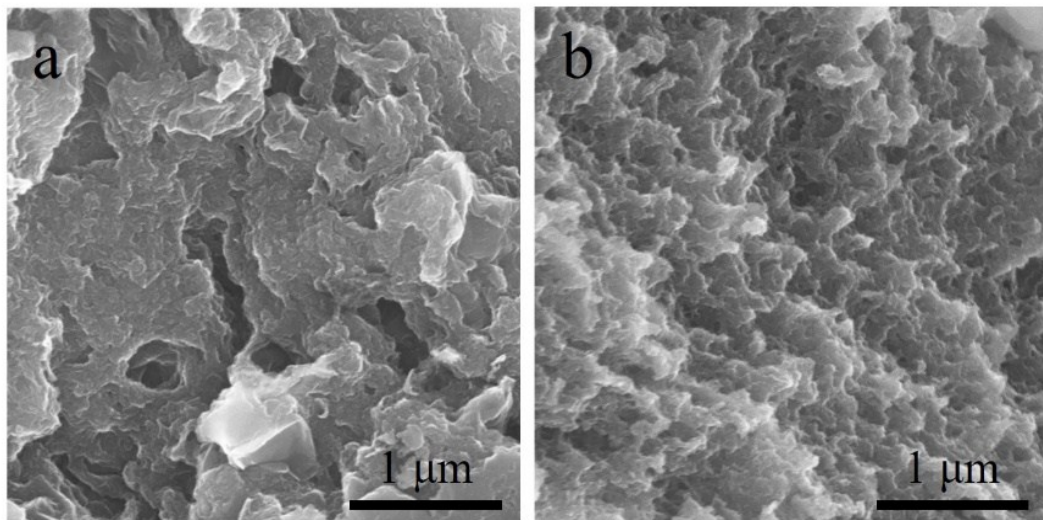


Fig. S2. SEM images of (a) pure NGO and (b) Pt₃Ni₇O-NGO.

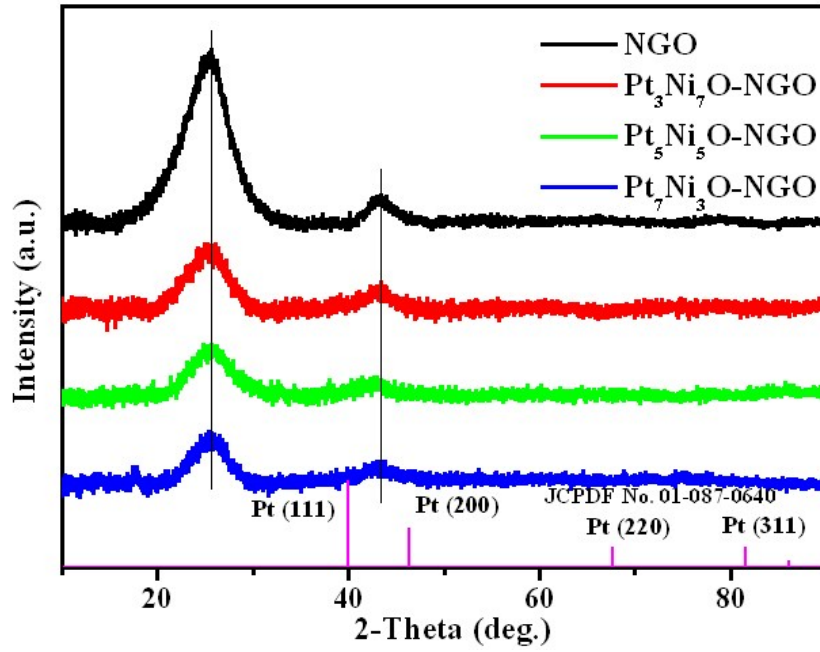


Fig. S3. XRD patterns of NGO and $\text{Pt}_x\text{Ni}_{10-x}\text{O}$ -NGO samples. The two broad diffraction peaks are attributed to NGO substrate. No obvious XRD peak can be observed for the $\text{Pt}_x\text{Ni}_{10-x}\text{O}$ NPs.

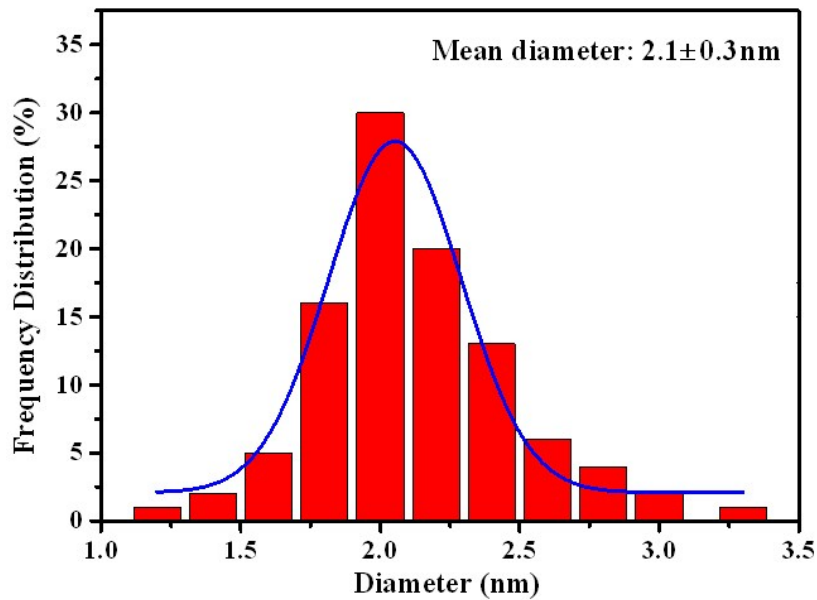


Fig. S4. The particle size distribution of $\text{Pt}_3\text{Ni}_7\text{O}$ -NGO with an average size of 2.1 nm.

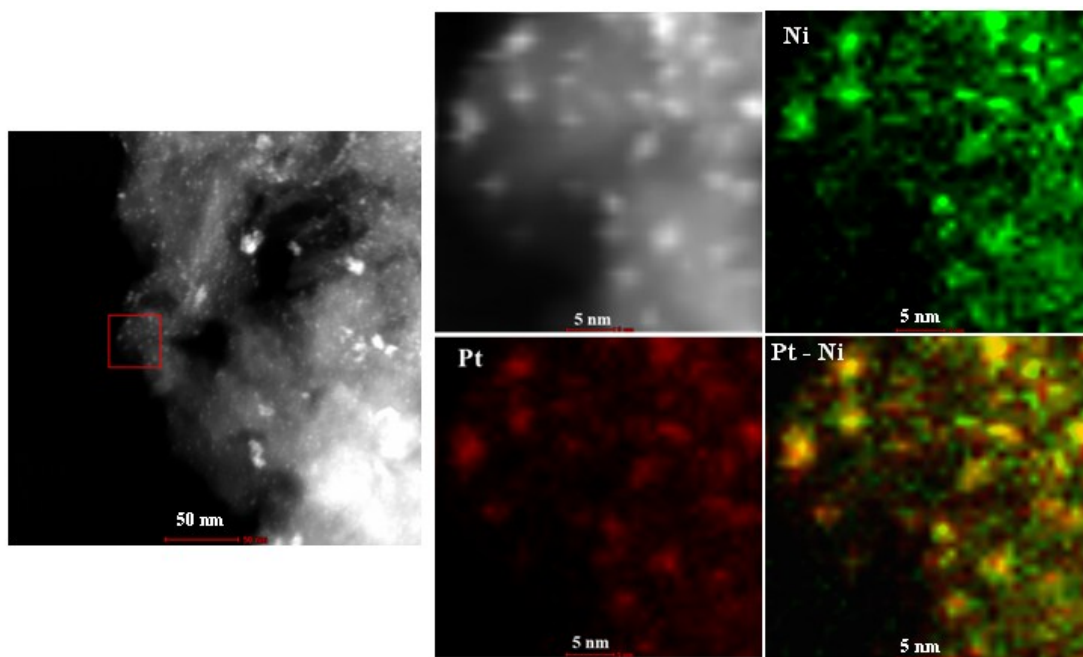


Fig. S5. Dark field TEM image and the high-resolution elemental mappings of $\text{Pt}_3\text{Ni}_7\text{O-NGO}$.

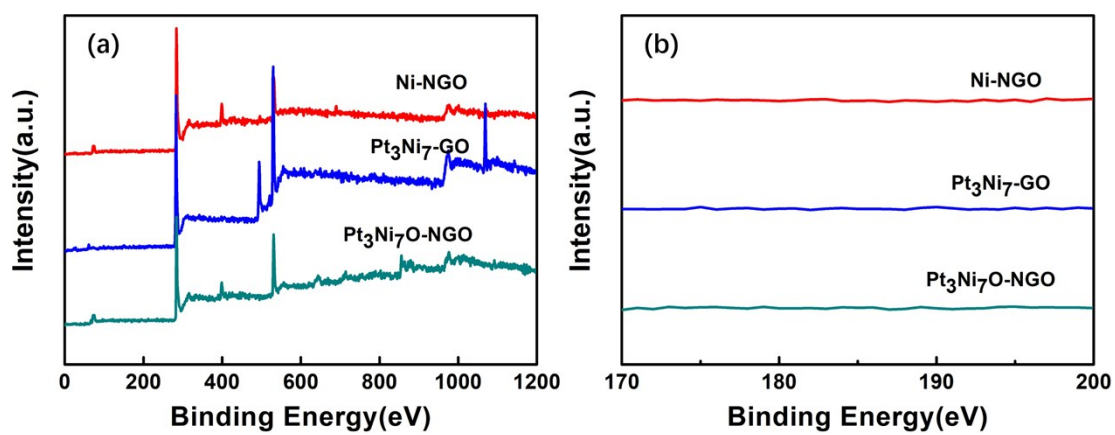


Fig. S6. XPS spectra of $\text{Pt}_3\text{Ni}_7\text{O-NGO}$, $\text{Pt}_3\text{Ni}_7\text{-GO}$ and Ni-NGO: (a) the survey spectra, (b) the high-resolution spectra at B 1s edge.

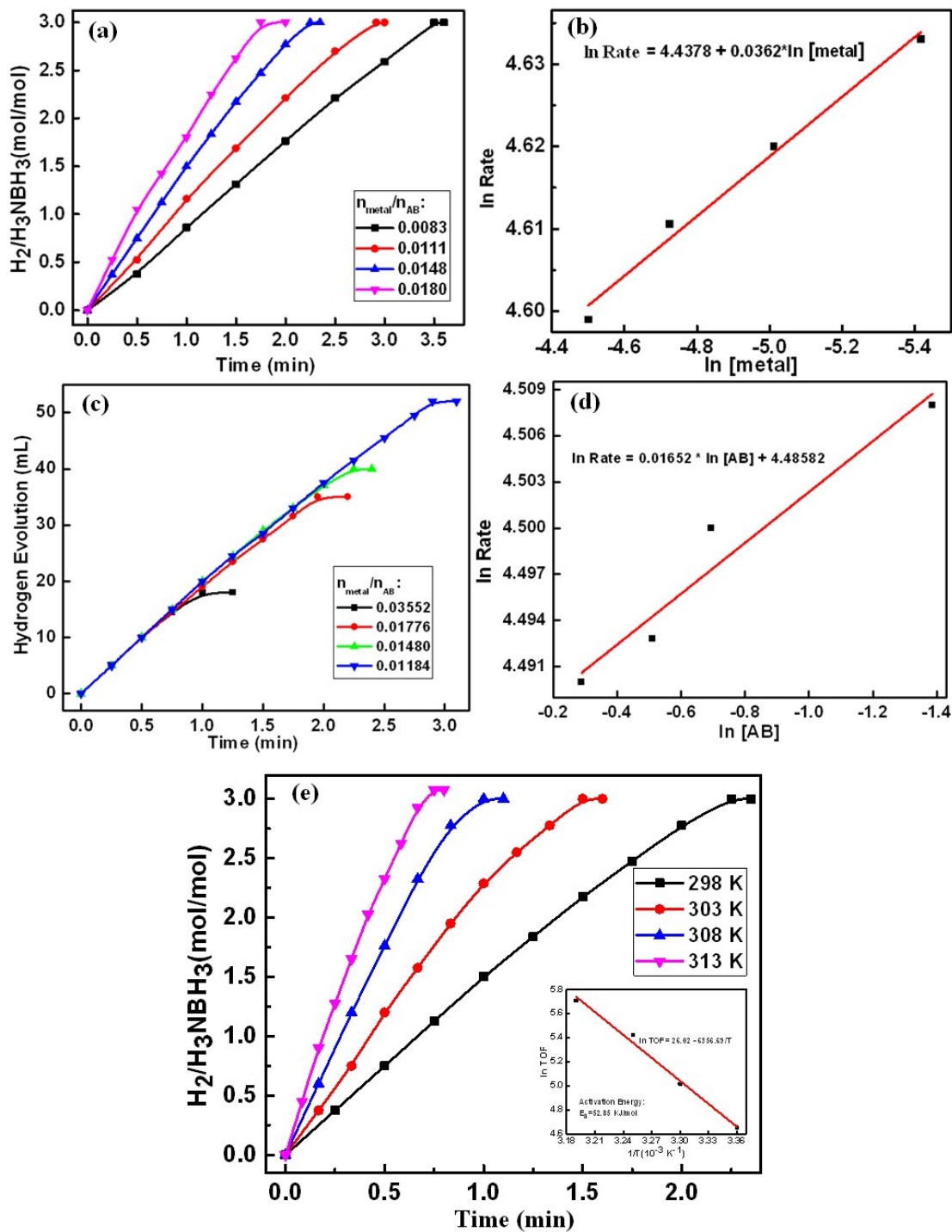


Fig. S7. (a) Stoichiometric hydrogen evolution in aqueous solution at a fixed amount of AB with various Pt₃Ni₇O-NGO/AB molar ratios at 298 K; (c) Relationship between hydrogen-generating rate and AB concentration at a fixed amount of Pt₃Ni₇O-NGO in aqueous solution at 298 K; (b) and (d): Logarithmic plots of rate versus [Pt₃Ni₇O-NGO] and [AB], respectively. (e) Hydrogen-generating rate as a function of temperature in the

hydrolysis of AB catalyzed by $\text{Pt}_3\text{Ni}_7\text{O-NGO}$. Inset: Arrhenius plot of $\ln(\text{TOF})$ versus $1/T$. The activation energy is calculated to be 52.85 kJ/mol.

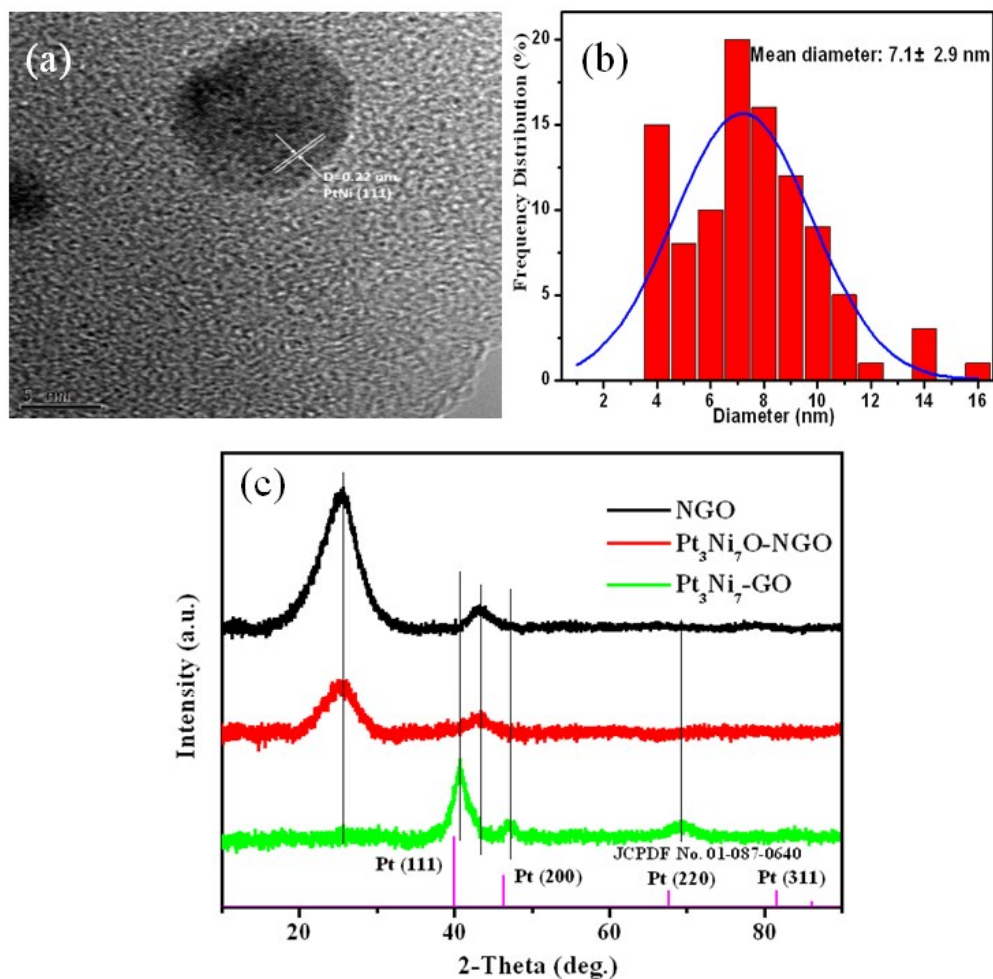


Fig. S8. TEM image (a), particle size distribution (b) and XRD pattern of $\text{Pt}_3\text{Ni}_7\text{-GO}$. The XRD patterns of NGO, $\text{Pt}_3\text{Ni}_7\text{O-NGO}$ and the standard Pt are shown for comparison.

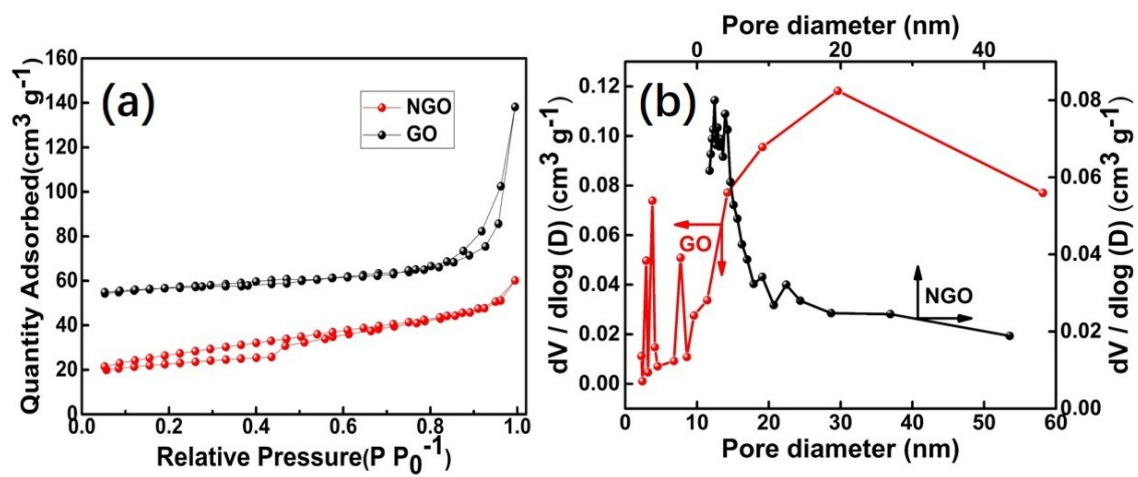


Fig. S9. (a) N₂ adsorption-desorption isotherms of NGO and GO at 77 K. (b) The corresponding pore size distributions of NGO and GO.

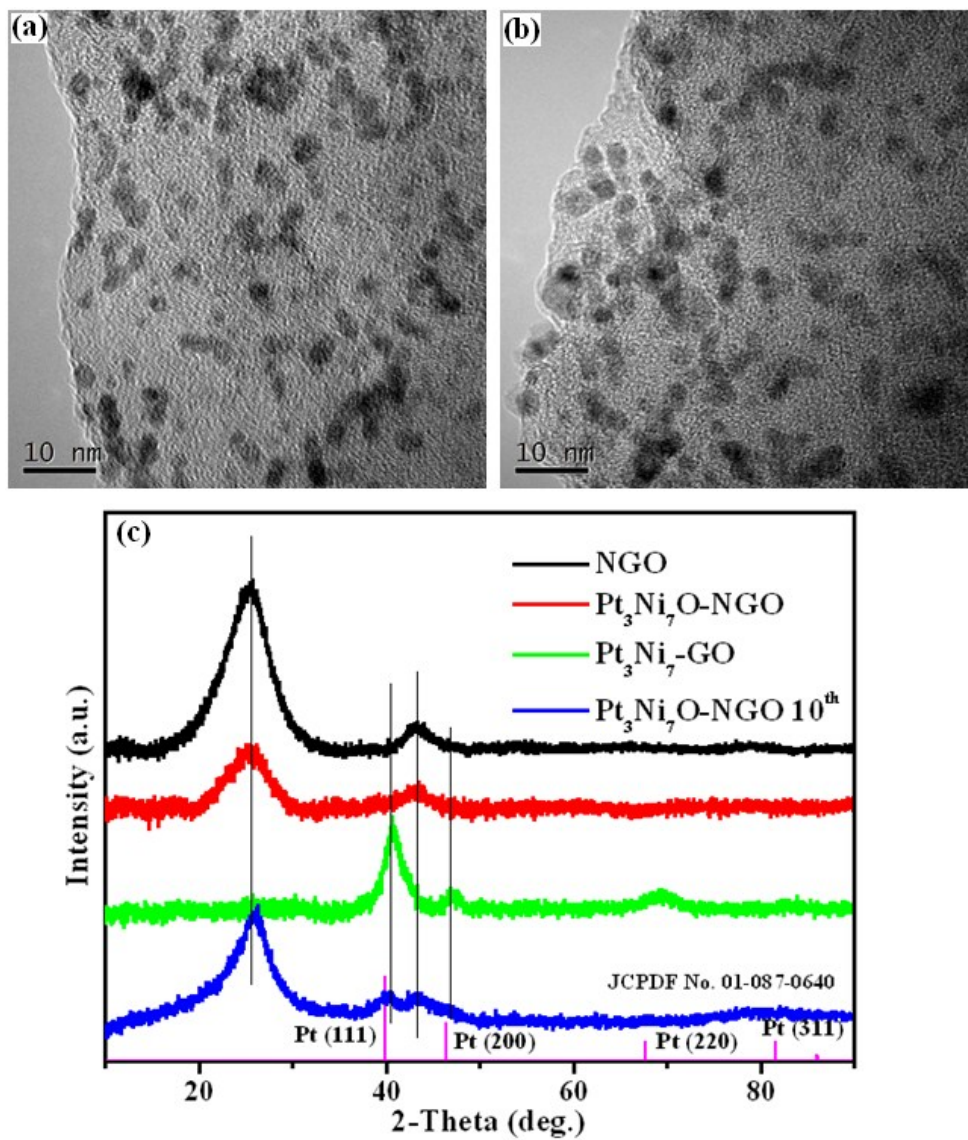


Fig. S10. (a) and (b): TEM images of the as-prepared Pt₃Ni₇O-NGO and Pt₃Ni₇O-NGO after 9 cycles (labeled as Pt₃Ni₇O-NGO 10th), respectively. (c) XRD patterns of NGO, Pt₃Ni₇O-NGO, Pt₃Ni₇-GO and Pt₃Ni₇O-NGO 10th.

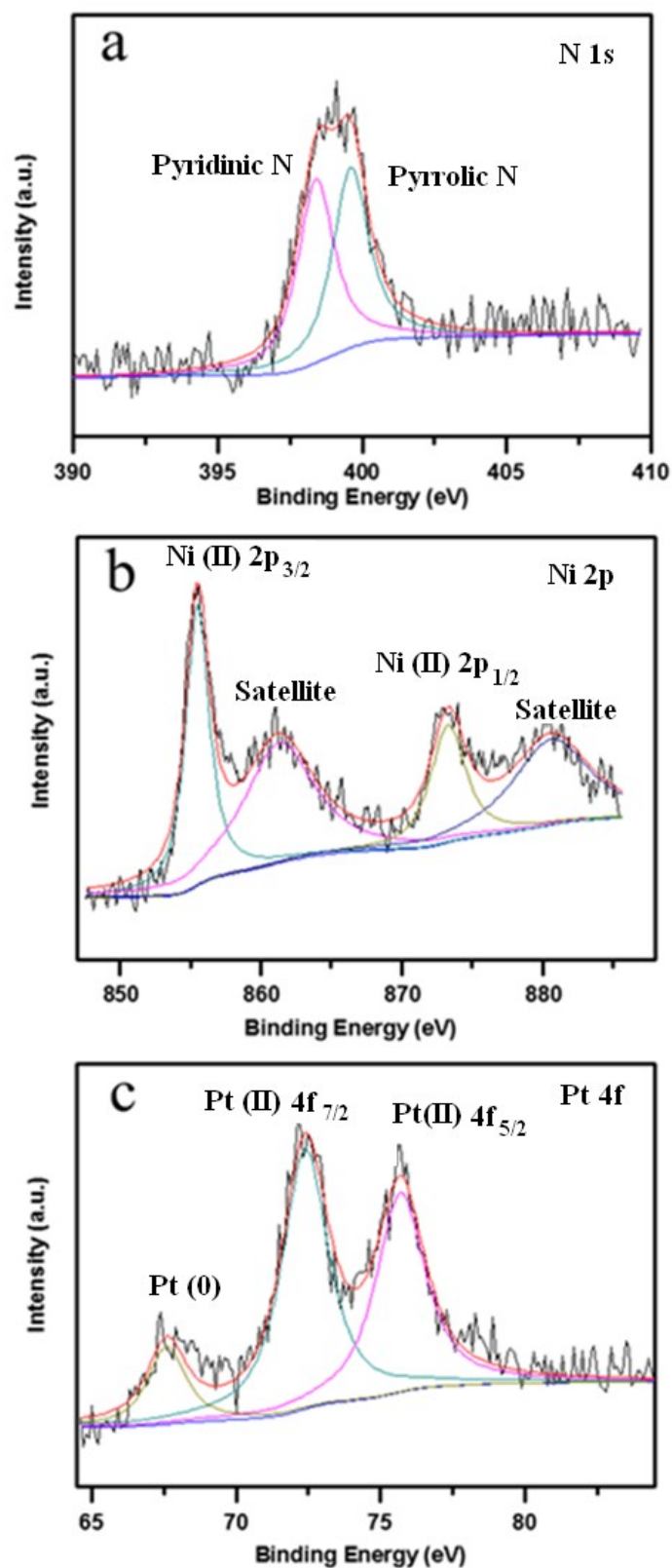


Fig. S11. XPS spectra of Pt₃Ni₇O-NGO at (a) N 1s, (b) Ni 2p, and (c) Pt 4f edges, respectively.

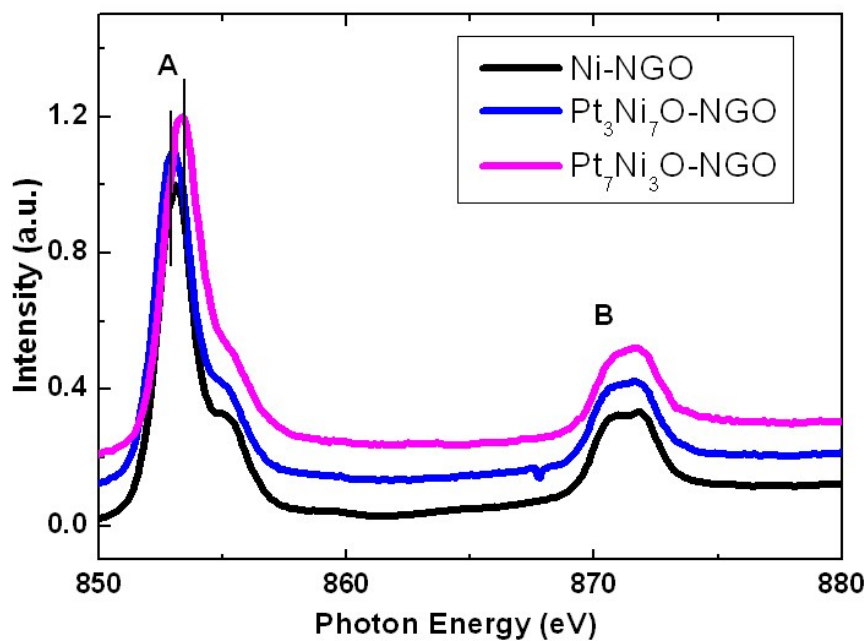


Fig. S12. Soft X-ray XAS spectra of Ni-NGO, Pt₃Ni₇O-NGO and Pt₇Ni₃O-NGO at Ni *L*-edge.

Samples	Pt-loading (wt%)	Ni-loading (wt%)	The atomic ratio of Pt and Ni	TOF (H ₂) mol/(Cat-M)mol·min	TOF (H ₂) mol/(Cat-Pt)mol·min
Pt ₃ Ni ₇ O-NGO	4.92	7.21	2:10	120.7	709.6
Pt ₅ Ni ₅ O-NGO	9.14	4.49	6.1:10	67.1	176.9
Pt ₇ Ni ₃ O-NGO	10.12	6.41	4.7:10	42.5	132.0
Pt ₃ Ni ₇ -GO	1.16	1.39	2.5:10	68.2	339.2
Ni-NGO	-	17.82	-	1.3	-
Pt-NGO	13.50	-	-	104.2	104.2
NGO	-	-	-	0	0

Table S1. Pt and Ni contents (measured by ICP-OES) and the TOF values of various Pt_xNi_{10-x}O-NGO, Pt₃Ni₇-GO, Ni-NGO, Pt-NGO and NGO samples.

Catalyst	TOF (H ₂) mol/(Cat-Pt)mol·min	T (°C)	Ref.
PtNi/NiO	1240.3	25	1
Pt ₃ Ni ₇ O-NGO	709.6	25	This work
Pt ₄ Ni ₁ @PVP NPs	638	25	2
Pt/CNTs-O-HT	468	25	3
Pt@MIL-101	414	25	4
PEI-GO/Pt _{0.17} Co _{0.83}	377.83	25	5
Pt-TiO ₂	311	25	6
G4-OH(Pt ₁₂ Ni ₄₈)	239.7	70	7
Pt/γ-Al ₂ O ₃	222.22	25	8
Pt/C	111	25	9
PtO ₂	20.8	25	9
Pt black	13.9	25	9

Table S2. Comparison of the TOF value of Pt-based catalysts for the hydrolysis of amine boranes in this work and those reported in the literatures.

References listed in Table S2:

1. Y. Ge, W. Ye, Z. H. Shah, X. Lin, R. Lu and S. Zhang, *ACS Appl. Mater. Interfaces*, 2017, **9**, 3749-3756.
2. S. Wang, D. Zhang, Y. Ma, H. Zhang, J. Gao, Y. Nie and X. Sun, *ACS Appl. Mater. Interfaces*, 2014, **6**, 12429-12435.
3. W. Chen, J. Ji, X. Duan, G. Qian, P. Li, X. Zhou, D. Chen and W. Yuan, *Chem. Commun.*, 2014, **50**, 2142-2144.
4. A. Aijaz, A. Karkamkar, Y. Choi, N. Tsumori, E. Rönnebro, T. Autrey, H. Shioyama and Q. Xu, *J. Am. Chem. Soc.*, 2012, **134**, 13926-13929.
5. M. Li, J. Hu, Z. Chen and H. Lu, *RSC Advances*, 2014, **4**, 41152-41158.
6. M. Khalily, H. Eren, S. Akbayrak, H. Akbayrak, N. Biyikli, S. özkar and M. Guler,

Angew. Chem. Int. Ed., 2016, **55**, 12257-12261.

7. K. Aranishi, A. Singh and Q. Xu, *ChemCatChem*, 2013, **5**, 2248-2252.

8. M. Chandra and Q. Xu, *J. Power Sources*, 2007, **168**, 135-142.

9. Q. Xu and M. Chandra, *J. Alloy Compd.*, 2007, **446-447**, 729-732.

Cycles	TOF (H ₂) mol/(Cat-Pt)mol·min	Catalytic Efficiency
1 st	709.6	100%
2 nd	681.2	96.0%
3 rd	627.8	88.5%
4 th	627.8	88.5%
5 th	584.7	82.4%
6 th	584.7	82.4%
7 th	544.9	76.8%
8 th	544.9	76.8%
9 th	544.9	76.8%
10 th	544.9	76.8%

Table S3. TOF values and the catalytic efficiencies of Pt₃Ni₇O-NGO in different cycles during the stability test.